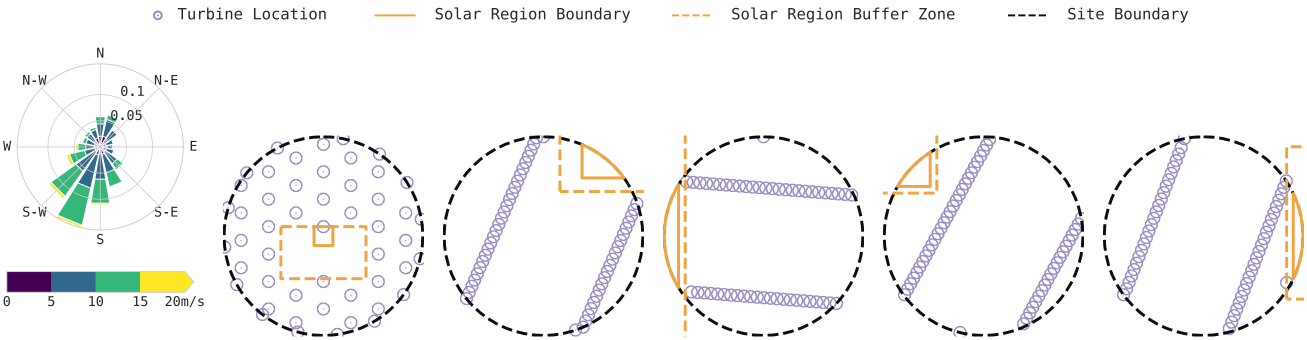

(a) Wind Rose (b) Baseline (c) Solution 1c (d) Solution 1d (e) Solution 1e (f) Solution 1f

Figure 1. CMA-ES solutions for the high-correlation location and circular boundary. Turbine locations are marked in purple, the solar region is drawn with an orange solid line, and the surrounding solar buffer zone is marked with a dashed orange line.

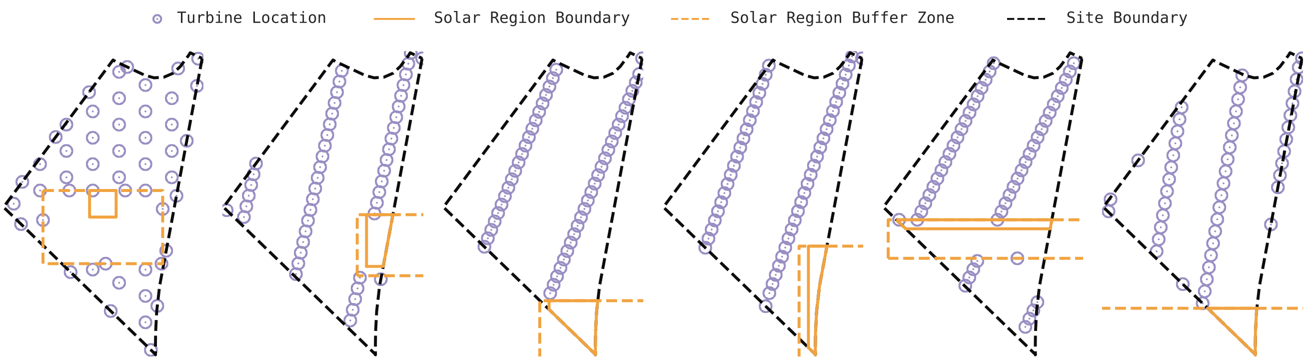

(a) Baseline (b) Solution 2b (c) Solution 2c (d) Solution 2d (e) Solution 2e (f) Solution 2f

Figure 2. CMA-ES solutions for the high-correlation location and irregular boundary.

0.1 A Closer Look at the Generated Layouts

Figures 1–4 show a sampling of solution layouts generated by CMA-ES using our hybrid layout parameterization. Each layout's performance statistics are listed in Table 1. In Figure 1, the high-correlation location and circular boundary generates a diversity of high-performing layouts. All these layouts pack all or all but one turbine into two inner grid rows, typically aligning turbine rows to an angle at a few degrees offset from the prevailing wind direction. This arrangement minimizes mean wake losses in our eddy viscosity-based wake loss simulation, causing wakes to fall just to the side of downstream turbines under most wind conditions. We also see some solutions, such as the layout shown in Figure 1c, that align the grid closer to perpendicular to the prevailing wind direction. This configuration is also competitive, but the closer spacing between rows in the wind direction results in the southerly turbines incurring a bit more wake losses. Similarly, the solver finds a variety of good solar placements, many of which are nonintuitive, including placements such as those shown in Figure 1c and Figure 1e, which place the solar region along the northern boundary of the site. Despite this northerly placement, the optimizer identified turbine placements that eliminate flicker losses.

Figure 2 shows solutions for the irregular boundary on the same high-correlation location. Unsurprisingly, these solutions share design characteristics with those using a circular boundary, but results differ in a few ways. The "taller" north-south aspect of the irregular boundary causes the optimizer to find solutions that align two and occasionally three rows of turbines with the longer chords of the boundary, again offsetting turbine rows a bit from the prevailing wind direction. Unlike with the circular boundary, some solutions place a smattering of turbines along the site boundary, taking advantage of the additional breathing room afforded by this boundary. In most cases, the solar is packed into the southern tip of the site, eliminating flicker losses

Table 1. CMA-ES layout performance statistics for each solution in Figures 1–4.

Location	Site	Solution	AEP GWh	Solar AEP GWh	Wind AEP GWh	Wake Loss	GCR Loss	Flicker Loss
High-Correlation	Circular	Baseline	214.29	101.36	112.93	4.15%	6.55%	0.09%
High-Correlation	Circular	5c	223.06	107.46	115.60	1.89%	1.02%	0.00%
High-Correlation	Circular	5d	222.08	107.46	114.62	2.72%	1.02%	0.01%
High-Correlation	Circular	5e	222.73	107.46	115.26	2.18%	1.02%	0.00%
High-Correlation	Circular	5f	222.76	107.46	115.30	2.15%	1.02%	0.00%
High-Correlation	Irregular	Baseline	211.78	101.36	110.43	6.28%	6.55%	0.10%
High-Correlation	Irregular	6b	220.94	107.45	113.48	3.69%	1.02%	0.01%
High-Correlation	Irregular	6c	220.98	107.46	113.52	3.66%	1.02%	0.00%
High-Correlation	Irregular	6d	221.04	107.46	113.58	3.61%	1.02%	0.00%
High-Correlation	Irregular	6e	220.65	107.36	113.29	3.85%	1.02%	0.10%
High-Correlation	Irregular	6f	220.36	107.46	112.90	4.18%	1.02%	0.00%
Low-Correlation	Circular	Baseline	159.02	103.57	55.45	5.38%	6.47%	0.08%
Low-Correlation	Circular	7c	165.21	109.09	56.12	4.24%	1.57%	0.00%
Low-Correlation	Circular	7d	165.16	109.09	56.07	4.32%	1.57%	0.00%
Low-Correlation	Circular	7e	165.22	109.09	56.13	4.22%	1.57%	0.00%
Low-Correlation	Circular	7f	165.20	109.09	56.10	4.26%	1.57%	0.00%
Low-Correlation	Irregular	Baseline	157.36	103.58	53.79	8.21%	6.47%	0.08%
Low-Correlation	Irregular	8b	164.40	109.07	55.34	5.57%	1.57%	0.02%
Low-Correlation	Irregular	8c	164.43	109.06	55.37	5.50%	1.57%	0.03%
Low-Correlation	Irregular	8d	164.43	109.06	55.37	5.50%	1.57%	0.03%
Low-Correlation	Irregular	8e	164.44	109.06	55.38	5.50%	1.57%	0.03%
Low-Correlation	Irregular	8f	164.44	109.06	55.38	5.50%	1.57%	0.03%

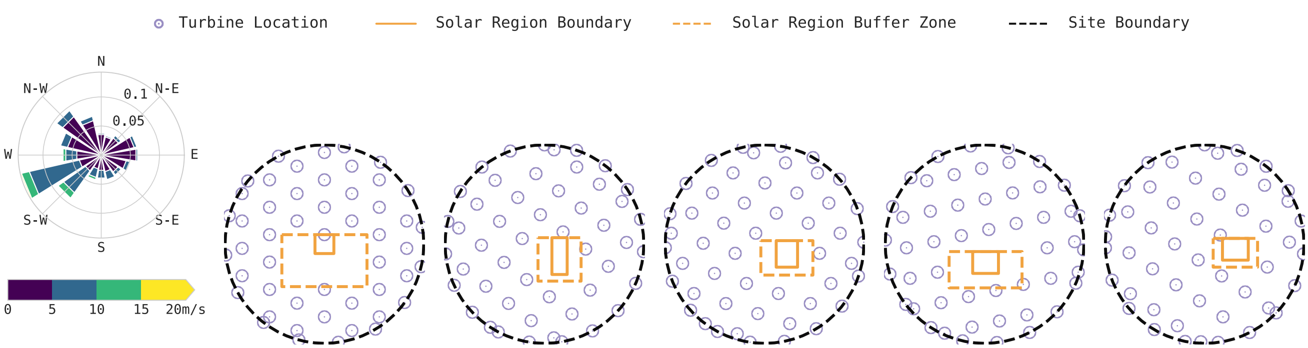

(a) Wind Rose (b) Baseline (c) Solution 3c (d) Solution 3d (e) Solution 3e (f) Solution 3f

Figure 3. CMA-ES solutions for the low-correlation location and circular boundary.

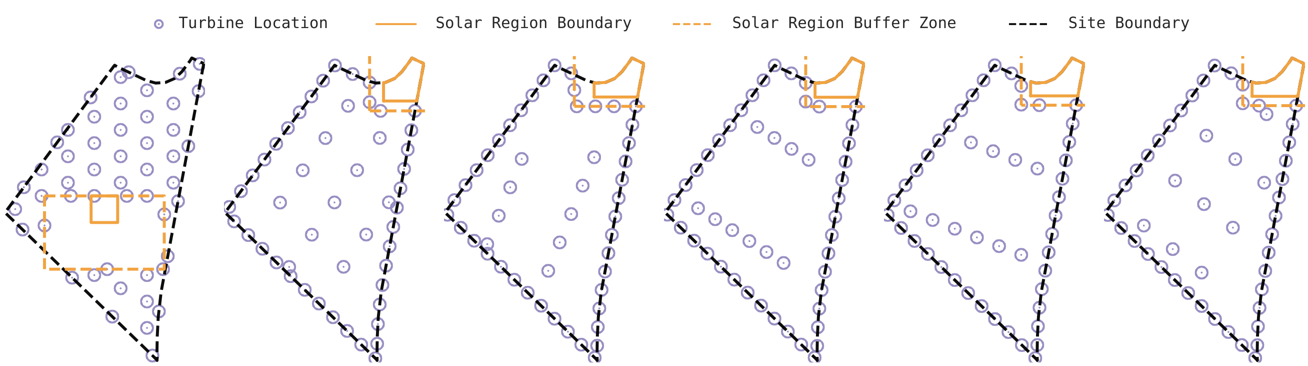

(a) Baseline (b) Solution 4b (c) Solution 4c (d) Solution 4d (e) Solution 4e (f) Solution 4f

Figure 4. CMA-ES solutions for the low-correlation location and irregular boundary.

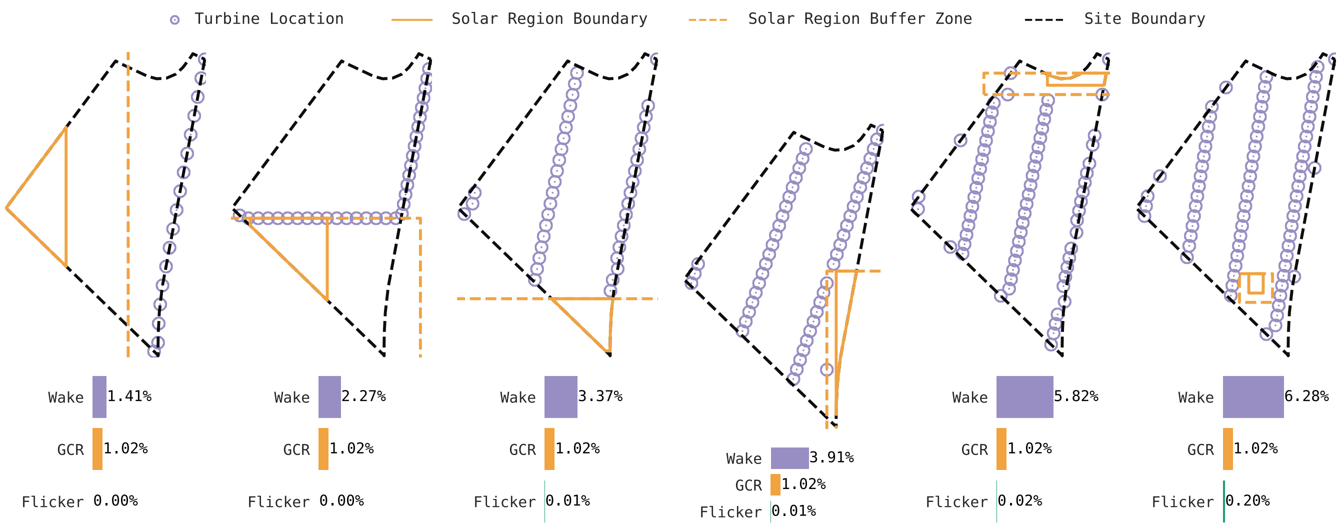

(a) 80% Solar (b) 60% Solar (c) 50% Solar (d) 40% Solar (e) 20% Solar (f) 10% Solar

Figure 5. Solutions generated for the high-correlation location and irregular boundary for a range of solar and wind capacity mixes, holding total nameplate capacity at 125MW.

entirely; however, a few competitive layouts were found that place the solar region deep in the site's interior, an interesting trade-off that increases turbine spacing at the cost of some flicker and shading losses.

The solutions shown in Figure 3 are generated layouts for the low-correlation location and circular boundary. Here, we see that the more uniform and lower speed wind distribution results in very different solutions than at the high-correlation location. In response to a less concentrated wind direction distribution, the solver proposes layouts that space turbines evenly and place the solar region near the site center, giving turbines some additional separation. Similar results are shown in Figure 4 using the irregular boundary, which primarily differ in an increased utilization of boundary turbines, and placement of the solar region into the northeastern corner of the site. These solutions are likely found because placing the solar in this corner actually causes boundary turbines to avoid the corner and therefore achieve increased spacing. A further-refined parameterization might specially handle border turbine placement in sharp boundary peninsulas such as this one. The ability to generate multiple competitive alternative layouts is a distinct advantage of evolution strategies and other stochastic optimization approaches. Here, we see the creative power of these solution methods in finding a large diversity of viable candidate layouts, all of which yield high objective function scores. In choosing to lay out a hybrid site, one might use these methods to generate a number of good candidate sites, and then choose among them based on other important factors that are difficult to encode in such an objective function, such as ease of access, maintenance or cabling concerns, aesthetics, and more.

0.2 Layouts for varying capacity mixes.

Figure 5 shows solutions for various solar to wind generation capacity proportions while holding total capcity equal to 125 MW. For solar-heavy specifications, turbines are placed where they will never shade the solar region, and are also spread out to minimize GCR losses, with reducing wake losses only a secondary concern. Figure 5b is a supprising layout which uses the solar region to position the turbines along two rows in a way which also yields low 2.27% wake losses for this location. As solar capacity is decreased and wind capacity is increased, the solar region naturally shrinks and is gradually placed to allow for reduced wake losses, with solar losses taking a back seat. Figure 5f shows a primarily wind-based layout with solar stuffed in-between two turbine rows almost as an afterthought. However, even in this case flicker losses are only 0.1% and the panels are rarely shaded.